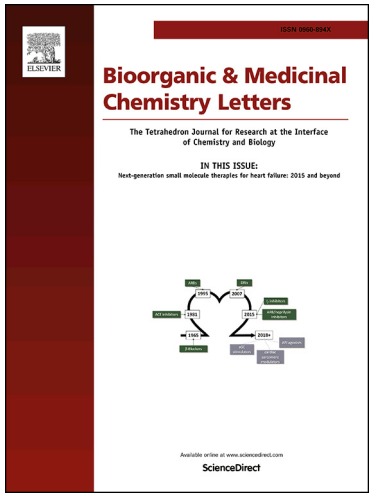

Discovery of novel 9H-purin derivatives as dual inhibitors of HDAC1 and CDK2

Yu Yu, Dongzhi Ran, Junhao Jiang, Tao Pan, Yanrong Dan, Qiang Tang, Wei Li, Lin Zhang, LinLing Gan, Zongjie Gan

PII: S0960-894X(19)30441-X
DOI: https://doi.org/10.1016/j.bmcl.2019.06.059
Reference: BMCL 26537

To appear in: *Bioorganic & Medicinal Chemistry Letters*

Received Date: 23 May 2019
Revised Date: 22 June 2019
Accepted Date: 28 June 2019

Please cite this article as: Yu, Y., Ran, D., Jiang, J., Pan, T., Dan, Y., Tang, Q., Li, W., Zhang, L., Gan, L., Gan, Z., Discovery of novel 9H-purin derivatives as dual inhibitors of HDAC1 and CDK2, *Bioorganic & Medicinal Chemistry Letters* (2019), doi: https://doi.org/10.1016/j.bmcl.2019.06.059

Discovery of novel 9H-purin derivatives as dual inhibitors of HDAC1 and CDK2

Yu Yu [a, b], Dongzhi Ran [a, b], Junhao Jiang [a, b], Tao Pan [a], Yanrong Dan [a], Qiang Tang [a, b], Wei Li [a, b], Lin Zhang [a], LinLing Gan [a], Zongjie Gan [a, b] *

[a] *Department of Medicinal Chemistry, College of Pharmacy, Chongqing Medical University, Chongqing 400016, PR China*

[b] *Chongqing Research Center for Pharmaceutical Engineering, Chongqing Medical University, Chongqing 400016, PR China*

*Corresponding author: ZongJie Gan

Email: gzj@cqmu.edu.cn

Tel.:86-23-68485161

Abstract HDAC and CDK inhibitors have been demonstrated to be synergistically in suppressing cancer cell proliferation and inducing apoptosis. In this work, we incorporated the pharmacophore groups of HDACs and CDKs inhibitors into one molecule to design and synthesize a series of purin derivatives as HDAC/CDK dual inhibitors. The lead compound **6d**, showing good HDAC1 and CDK2 inhibitory activity with IC_{50} values of 5.8 and 56 nM, respectively, exhibited attractive potency against several cancer cell lines in vitro. This work may lead to the discovery of a novel scaffold and potential dual HDAC/CDK inhibitors.

Keywords HDACs; CDKs; Dual inhibitors; Purin; Antitumor

Histone deacetylases (HDACs) are a family of enzymes which could catalyze the removal of acetyl groups from the ε-amino groups of lysine residues presenting within the N-terminal extension of the core histones.[1] Such modifications are crucial for the regulation of gene expression and cellular processes, including apoptosis, cell growth and differentiation.[2,3] However, aberrant histone deacetylation, owing to the increased activity and expression of HDACs ~~activity and expression~~, has been demonstrated in several kinds of cancer cell lines and correlated with aggressiveness, migration and invasion of cancer.[4,5] Thus, inhibition of HDACs has proven to be a valuable epigenetic strategy for cancer treatment. Over the past decade, there have been intense efforts to identify novel small-molecule HDACs inhibitors to address unmet medical needs. Up to now, there are already approved HDACs inhibitors such as SAHA and panobinostat for the treatment of lymphoma and multiple myeloma (Fig. 1).[6,7] Despite the efficacy in hematological malignancies, HDACs inhibitors as monotherapy in solid tumors have been proved less effective than hematological malignancies in vivo ~~and~~ thus combination of HDACs inhibitors with other anticancer agents may result in the improved anti-proliferation of tumor cells, which represents a new therapeutic approach to ~~the~~ malignancies treatment. [8-10]

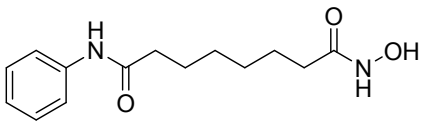

SAHA

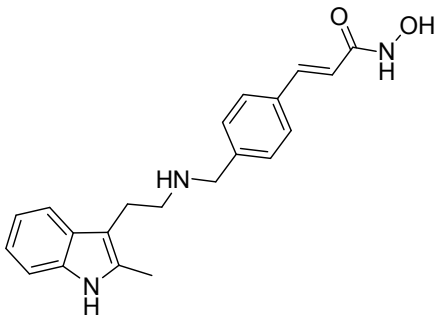

Panobinostat

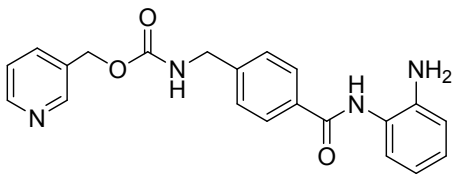

Entinostat

Figure 1. Structures of the approved HDACs inhibitors.

Cyclin-dependent kinases (CDKs) are key regulators of cell division cycle, since CDKs are often deregulated in cancer, thus, CDKs inhibitors which target CDKs are considered to be a promising agent for cancer treatment.[11] Recently, studies have indicated that the inhibition of CDKs sensitizes cancer

cells to HDACs inhibitors which could induce apoptosis, thus combination of HDACs and CDKs inhibitors may have statistically synergy in suppressing cancer cell proliferation. For instance, Gahr and coworkers[12] have reported that the combination of HDACs inhibitor entinostat with CDKs inhibitor roscovitine could inhibit the cell cycle progression and increase the suppression of hepatoma cell DNA synthesis. Furthermore, the synergistic combination between the inhibitors of CDKs and HDACs was proved to overcome CDKs inhibitor resistance by activating p21 in ER-positive breast cancer cells, which might be beneficial in the resistant cases of CDKs inhibitors.[13] Therefore, following the success of synergy between HDACs and CDKs inhibitors, we conceived that the incorporation of ~~the~~ pharmacophore groups of HDACs and CDKs inhibitors into one molecule for the concurrent inhibition of HDACs and CDKs would be an effective way to optimize HDACs and CDKs inhibitors' efficacy in solid tumors and avoid unwanted side effects associated with the combination therapy, such as drug-drug interaction, different physicochemical properties, or poor patient compliance. Lately, Xiang et al[14] have reported a series of 7H-pyrrolo[2,3-d]pyrimidine derivatives bifunctional targeting on CDK4/9 and HDAC1, which demonstrated excellent antitumor efficacy against 4T1 tumor xenograft models in vivo, suggesting the development of CDK/HDAC dual inhibitors could be of great significance for malignant cancer therapy.

According to the crystal structure of CDK2 complexed with its selective analog roscovitine, [15] it is found that the purin group of roscovitine occupies the ATP binding pocket, functioning as the mainly binding moiety with ATP. On the other hand, it is well known that the pharmacophore of HDACs inhibitors comprises three parts, including a zinc-binding group (ZBG), a linker and a surface recognition "CAP" group.[16] Generally, the CAP region is predominantly responsible for selectivity and tolerates a large change. Therefore, we have chosen purin ring instead of indole ring as the "CAP" group, utilized ethenylphenyl as the linker to link the ZBG and CAP groups with the aim to discover novel HDAC/CDK dual inhibitors (Figure 2). With this approach, a novel scaffold and potential HDAC/CDK dual inhibitor has been designed and presented in this work.

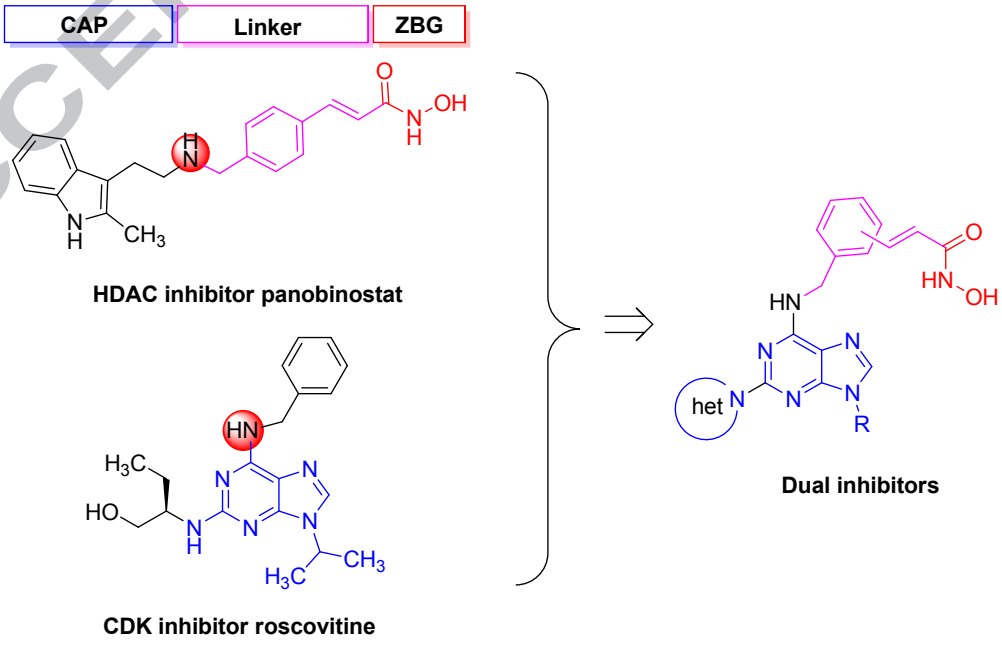

Figure 2. Design strategy of HDAC/CDK dual inhibitors.

The preparation of target compounds (**6**) was described in Scheme **1**. The target compounds were synthesized from commercially available starting material 2, 6-dichloro-9H-purin (**1**) via a novel and convenient route. Reaction of (**1**) with corresponding iodoalkanes in DMF afforded intermediate (**2**), which was then condensed with 3- or 4-bromobenzyl amine under mild conditions providing intermediate (**3**). The intermediates (**4**), synthesized by the substitution of (**3**) with heterocyclic amines such as morpholine or piperidine, underwent standard Heck coupling with methyl acrylate in the presence of $Pd(OAC)_2$ to give the key intermediate (**5**). Finally, the ester groups of (**5**) reacted with freshly prepared hydroxylamine in methanol to produce target compounds (**6**). The aniline substituted compounds 6s-6t were prepared in the same way from the distinct reagent 4-bromoaniline in step b.

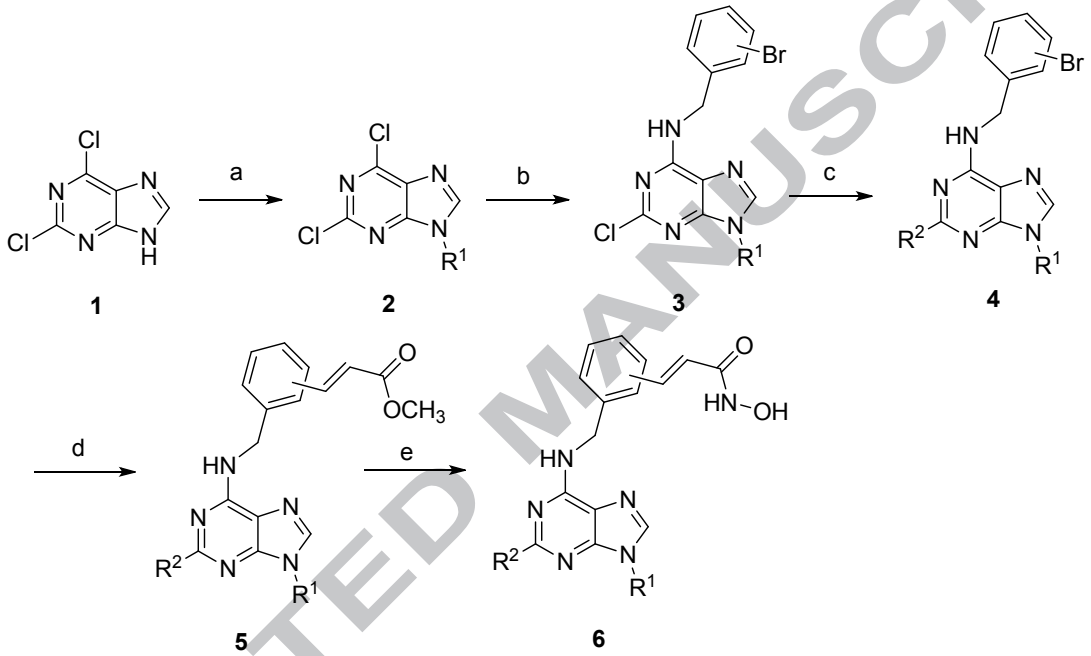

Scheme 1. *Reagents and conditions*: a) iodoalkanes, K_2CO_3, DMF, 0°C to rt, 10 h; b) 3- or 4-bromobenzyl amine, K_2CO_3, DMF, 90°C, 4 h; c) heterocyclic amines, 90°C, 3 h; d) methyl acrylate, $Pd(OAc)_2$, tri(o-tolyl)phosphine, CH_3CN, DMF, 90°C, 6 h; e) NH_2OH, KOH, CH_3OH, 0°C, 2 h.

To explore the biological profile, all synthesized compounds were evaluated against HDAC1 and CDK2 enzymes, and panobinostat, SAHA and roscovitine were employed as the positive control. The results are summarized in Table 1 as follows: despite the decreased activities comparing to the positive control panobinostat, all target compounds still demonstrated good inhibitory activities against HDAC1 at the concentrations of 10 nM and 1000 nM, while some of them could also inhibit CDK2 over 50% at 100 nM, indicating that most of these compounds are dual inhibitors. Among these derivatives, compound **6d** exhibited the most potent activities on CDK2 (IC_{50} = 56 nM), which was 4-fold more potent than roscovitine (IC_{50} = 192 nM), and also showed a remarkable function against HDAC1 (IC_{50} = 5.8 nM). Furthermore, in order to investigate the effects of substituents at R2 group on the HDAC1 and CDK2 inhibition, compounds **6a**, **6b, 6c** and **6n** were synthesized. The results showed that the replacement of morpholine by pyrrolidine, piperidine N-methylpiperazine and 4-methylpiperidine led to a decreased CDK2 inhibition, indicating that the morpholine group at R2 position is favorable for CDK2 inhibition, and similar trends were observed in compounds **6e, 6r, 6s**. In addition, with the

increasing size of R1 (**6e - 6g**), the inhibitory activity dramatically decreased, indicating that the substituted group at R1 position was critical for its activity and ethyl group at R1 position seemed to be optimal for CDK enzyme inhibitory activity. Interestingly, conversion of benzyl substituent to phenyl group barely influenced the CDK2 or HDAC1 inhibitory activity (**6s, 6t**). Deserved to be noted, unlike panobinostat, the compound **6e**, which possess an ortho-aniline group instead of a para-aniline (**6i**), showed higher binding affinity for HDAC1 probably due to the steric hindrance.

Table 1. Inhibition ratio of target compounds on HDAC1 and CDK2.

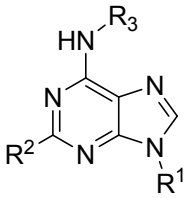

Compd.	R1	R2	R3	Inh% (HDAC1)		IC_{50} (nM)	Inh% (CDK2)		IC_{50} (nM)
				10 nM	1000 nM		10 nM	100 nM	
6a	**Et**	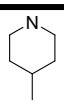	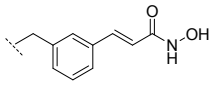	-	-	-	-2.7	22.5	-
6b	**Et**		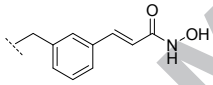	46	99	-	6.9	37.2	-
6c	**Et**		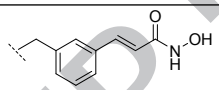	-	-	-	5.6	28.3	-
6d	**Et**		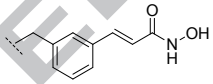	66	97	5.8	9.5	67.9	56
6e	**i-Pr**		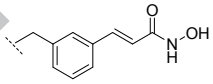	63	98	7.0	4.1	47.5	127
6f			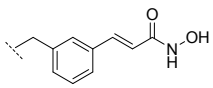	41	97	-	2.0	33.0	-
6g	**n-Bu**		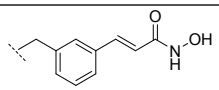	46	98	-	3.8	11.0	-
6h	**Me**		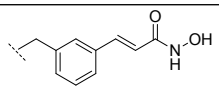	-	-	-	13.8	20.8	-
6i	**i-Pr**		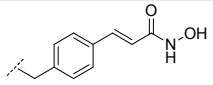	26	97	-	-	-	-
6j	**i-Pr**		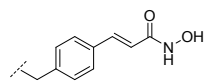	-	-	-	0.8	11.6	-
6k	**Me**		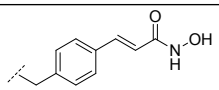	42	100	-	-7.4	1.6	-
6l	**i-Pr**		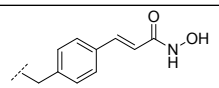	31	99	-	-1.2	3.7	-

6m	**Me**		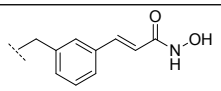	-	-	-	11.5	16.8	-
6n	**Et**		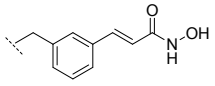	-	-	-	4.4	15.5	-
6o	**i-Pr**		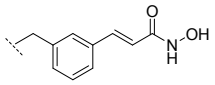	69	101	-	-12.1	21.7	-
6p	**n-Bu**		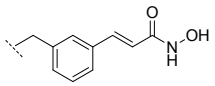	-	-	-	2.3	4.6	-
6q	**i-Pr**		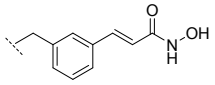	-	-	-	6.6	12.1	-
6r	**i-Pr**		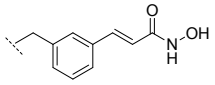	58	99	-	-0.8	5.0	-
6s	**i-Pr**		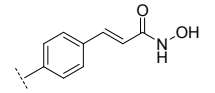	47	100	-	-15.4	15.2	-
6t	**Me**		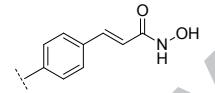	-	-	-	3.4	5.3	-
SAHA	-	-	-	46	100	-	-	-	-
Panobinostat	-	-	-	-	-	0.6	-	-	-
roscovitine	-	-	-	-	-	-	-	-	193

- Not determined

Encouraged by the favorable enzymatic potency, compounds **6d** and **6e** were selected to evaluate their growth inhibitory activities against several human tumor cell lines, including human lung cancer cells (A549), human liver cancer cells (HepG2) and human breast cancer cells (CAL-148). As shown in table 2, though less efficient than the panobinostat, compound **6d** and **6e** still inhibited the proliferation of all the tested cell lines at good degrees of inhibitory activities. HepG2 cell line seemed to be more sensitive than A549 and CAL-148 lines, and compound **6d** (IC_{50} = 0.77 ± 0.07 μM) and **6e** (IC_{50} = 0.22 ± 0.08 μM) exhibited better anti-proliferative activities than roscovitine revealing their potential for further modification.

Table 2. Cell growth inhibitory activities of compounds on human cancer cell lines.

Compd.	**IC_{50} (μM)** [a]		
	A549	**HepG2**	**CAL-148**
6d	1.49 ± 0.07	0.77 ± 0.07	1.14 ± 0.21
6e	1.26 ± 0.02	0.22 ± 0..08	0.39 ± 0..01
Panobinostat	0.02 ± 0.001	< 0.1	< 0.1
Roscovitine	>10	15.76 ± 3.09	>10

[a] Data are mean ± SD values from three independent experiments.

To elucidate the interaction mode of compound **6d**, the docking studies of **6d** in HDAC1 (PDB code: 4BKX) and CDK2 (PDB code: 2A4L) were performed on software Discovery Studio 2018 (Fig. 3). Figure 3A showed the binding mode of **6d** with the active site of HDAC1. Unsurprisingly, the hydroxamic acid group chelated the Zn^{2+} in a coordinated manner and formed hydrogen bonds. Meanwhile, the aliphatic linker occupied the lipophilic tube, and the cap group extended to a pocket and interacted with the amino acid residues Pro29 and His28. On the other hand, as shown in the binding mode of **6d** with CDK2 in Figure 3B, the purin moiety of **6d** occupied approximately the same ATP-binding region of CDK2 as the purin ring of roscovitine. Ethyl group on the morphine ring formed hydrophobic interactions with the residue Ala144 and Phe80, which was similar to the isopropyl group in roscovitine. It is worth noting that the hydroxamic acid group also formed strong hydrogen bond interactions with Glu8 and Lys20 residues, which may be the key contributor to the high potency of **6d** against CDK2 compared to roscovitine.

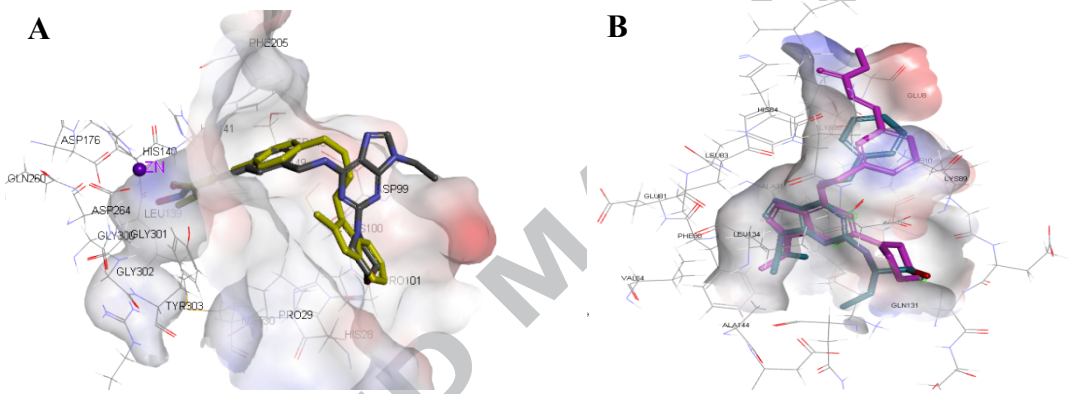

Fig 3. (A) The binding mode of compound **6d** (purple) and panobinostat (yellow) in the active site of HDAC2 (PDB code: 4BKX). (B) The binding mode of compound **6d** (purple) and roscovitine (green) in the active site of CDK2 (PDB code: 2A4L).

In conclusion, a series of fused-purin based novel HDAC1/CDK2 dual inhibitors were designed, synthesized, and evaluated for bioactivity. The growth inhibitory activities of synthesized compounds were tested using three human tumor cell lines. The potent lead compound **6d** with good HDAC1 and CDK2 inhibitory activity of IC_{50} = 5.8 and 56 nM, respectively, can effectively induce apoptosis of these cancer cell lines in vitro, especially on HepG2 cell line. Above studies supported **6d** as a good and novel candidate compound targeting on HDAC1 and CDK2, which deserved further research.

Acknowledgements

We appreciate the financial support from National Natural Science Foundation of China (No. 21701018) and the Natural Science Foundation of Chongqing City (No. cstc2017jcyjAX0228).

References

1. Bolden JE, Peart MJ, Johnstone RW. *Nat Rev Drug Discov*. 2006; 5: 769.
2. Khan O, La Thangue NB. *Immunol Cell Biol*. 2012; 90: 85.
3. Zhang Y, Feng J, Jia Y, et al. *J Med Chem*. 2011; 54: 2823.
4. Korfei M, Skwarna S, Henneke I, et al. *Thorax*. 2015; 70: 1022.
5. Park SY, Jun JA, Jeong KJ, et al. *Oncol Rep*. 2011; 25: 1677.
6. Muller S, Kramer OH. *Curr Cancer Drug Targets*. 2010; 10: 210.

7. Andrews KT, Haque A, Jones MK. *Immunol Cell Biol*. 2012; 90: 66.
8. Lachenmayer A, Toffanin S, Cabellos L, et al. *J Hepatol*, 2012; 56: 1343.
9. Shao M, He L, Zheng L, et al. *Bioorg Med Chem Lett*. 2017; 27: 4051.
10. Santos, F P. Verstovsek, S. *Curr Opin Hematol*. 2013; 20: 123.
11. Indovina P. *Curr Pharm Design*. 2013; 19: 5327.
12. Gahr S, Peter G, Wissniowski TT, et al. *Oncol Rep*, 2008; 20: 1249.
13. Lee J, Lim B, Pearson T, et al. *Cancer Res*. 2018; 78: P5.
14. Li Y, Luo X, Guo Q, et al. *J Med Chem*. 2018; 61: 3166.
15. Azevedo WFD, Leclerc S, Meijer L, et al. *Eur J Biochem*. 1997; 243: 518.

Graphical abstract:

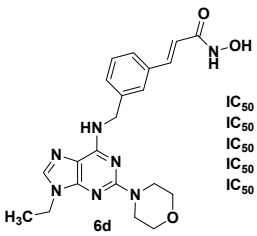

IC_{50} (HDAC1) = 5.8 nM
IC_{50} (CDK2) = 56 nM
IC_{50} (HepG2) = 0.77 ± 0.07 μM
IC_{50} (CAL-148) = 1.14 ± 0.21 μM
IC_{50} (A549) = 1.49 ± 0.07 μM

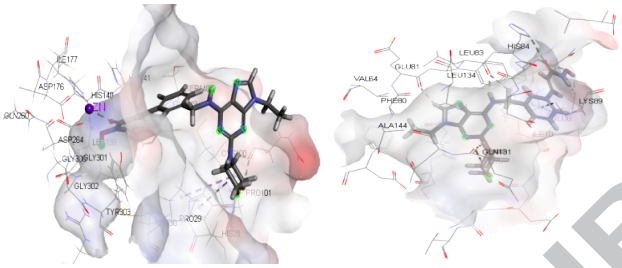

16.